

Optical properties of boron-doped diamond

Dan Wu, Y. C. Ma, Z. L. Wang, Q. Luo, C. Z. Gu, and N. L. Wang*

*Beijing National Laboratory for Condensed Matter Physics,
Institute of Physics, Chinese Academy of Sciences, Beijing 100080, China*

C. Y. Li, X. Y. Lu, Z. S. Jin

State Key Laboratory for Superhard Materials, Jilin University, Changchun 130021, PR China

(Dated: May 24, 2019)

We report optical reflectivity study on pure and boron-doped diamond films grown by a hot-filament chemical vapor deposition method. The study reveals the formation of an impurity band close to the top of the valence band upon boron-doping. A schematic picture for the evolution of the electronic structure with boron doping was drawn based on the experimental observation. The study also reveals that the boron doping induces local lattice distortion, which brings an infrared-forbidden phonon mode at 1330 cm^{-1} activated in doped sample. The antiresonance characteristic of the mode in conductivity spectrum evidences the very strong coupling between electrons and this phonon mode.

PACS numbers: 74.25.Gz ,71.55.Eq, 71.30.+h

Since diamond was used as an attractive material in many applications for its high hardness and stable chemical property, lots of studies have been done on diamond's transport and thermal properties. Pure diamond is a wide-gap semiconductor with the band gap of 5.5 eV.[1, 2] As the inspiration of adding impurity to semiconductor like silicon, the microwave plasma chemical vapor deposition (MPCVD) method as well as high pressure high temperature(HPHT) synthesizing skills are popularly used recently to add dopants into pure diamond, with the purpose to find out how impurities play roles in diamond.[3, 4] The most attractive impurity now should be boron as single electron acceptors. As the boron doping level increasing, a gradual change from a semiconductor to a metal, eventually to a superconductor occurs. Doped boron atoms substitute for the carbon atoms when the concentration is low $\leq 0.5\%$, and occupy neutrally interstitial positions at the doping level $\sim 4\%$. In low doping case, the substituted boron atoms are bonded to neighboring carbon atoms in the sp^3 environment, and in the ground state the holes provided by boron atoms are bound in one of the three fold degenerate impurity state with a binding energy of 0.38 eV. At higher boron concentration, as the average distance between boron atoms is close to the acceptor Bohr radius, the metallic conduction appears, with the room temperature conductivities of a few $10^2\text{ }\Omega^{-1}\text{cm}^{-1}$.[5, 6, 7]

The superconductivity of boron doped diamond at several Kelvins is now the most interesting phenomenon.[8, 9] In order to understand the origin of this phenomenon, a number of first-principle calculations have been performed recently with regard to the electronic structure, lattice dynamics, and the electron-phonon coupling of

the doped system.[10, 11, 12, 13] It was suggested that the superconductivity is mediated through the electron-phonon interaction. Holes doped at the top of the zone-centered, degenerate σ -bonding valence band couple strongly to the optical bond-stretching modes, a mechanism similar to the one causing the superconductivity in MgB_2 .[10] However, there is also a suggestion by Baskaran that an additional metallic "mid-gap band" of a conducting 'self-doped' Mott insulator contributes to the superconductivity.[14]

In this paper, we study the optical property of lightly boron doped diamond which has p-type semiconductor character and pure diamond films in a wide range of frequency with the temperature changing from 300 K to 10 K. A transfer of spectral weight from interband transition to the low frequencies was clearly observed, which provides experimental evidence for the evolution of the electronic structure with boron doping. A schematic picture was drawn based on the experimental observation. In addition, an antiresonance phonon feature is clearly observed at low-frequency $\sim 1330\text{ cm}^{-1}$ for boron-doped compound, indicating (1) the boron induced distortion is evident, which thus brings this infrared-forbidden mode activated in doped sample; (2) strong electron-phonon coupling.

The boron doped polycrystalline diamond thick film was grown using an hot-filament chemical vapor deposition (HFCVD) method on molybdenum substrates. The molybdenum substrates were ultrasonically pretreated in an ethanol solution containing diamond powder, followed by a -200 V bias voltage-assisted HFCVD process. In addition to the CH_4 and H_2 used as reaction gases, boron species were incorporated into the diamond films during the growth process by bubbling the H_2 gas (10 sccm) through the $\text{B}(\text{OCH}_3)_3$ liquid precursors at room temperature. The total pressure was 50 Torr and the substrate temperature was about 1073K measured by a thermocouple mounted on the substrate. After deposition of 60

*Corresponding author; Electronic address:
nlwang@aphy.iphy.ac.cn

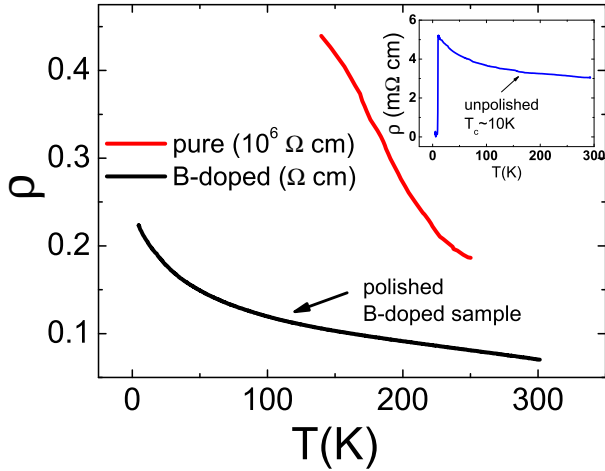


FIG. 1: (color online) The dc resistivity as a function of temperature for a pure and a boron-doped diamond film. Unpolished boron doped sample exhibits a superconducting transition near 10 K (Inset of the figure). The superconductivity was lost unexpectedly after polishing.

hours, the molybdenum substrates were removed by a cooling technique, and a freestanding diamond film with the thickness of about 100 μm was obtained. The scanning electron microscopy image indicates that the average diamond grain's size in the polycrystalline diamond thick film is larger than 10 μm . X-ray diffraction (XRD) measurement confirmed the pure phase and, to some degree, the preferred (111) orientation of the diamond film. The dc resistivity was measured by standard four probe method. Fig. 1 shows the resistivity vs T curves for pure and doped films. For the heavily doped sample, the resistivity value is much lower than the pure sample, and becomes superconducting below ~ 10 K.

The polycrystalline diamond films have very rough surfaces due to the different growth orientations of diamond grains. For optical reflectance measurement, the surface has to be polished. Unexpectedly, for some unknown reasons, we found the superconducting sample lost its superconductivity after being polished. The ρ -T curve of the same, but polished sample is also shown in Fig. 1. The near-normal incident reflectance spectra were measured by a Bruker 66 v/s spectrometer in the range from 40 to 25000 cm^{-1} and by a home-made grating spectrometer from 25000 cm^{-1} to 50000 cm^{-1} . The sample was mounted on an optically black cone in a cold-finger flow cryostat. An *in situ* overcoating technique was employed for reflectance measurements.[15] We performed Kramers-Kronig transformation of $R(\omega)$ to obtain the optical conductivity spectra. For the low frequency extrapolation, we use constant and Hagen-Rubens relation for pure and doped samples, respectively. At high frequency side, above the maximum frequency in the data file, the reflectance is extrapolated as ω^{-1} up to 400,000 cm^{-1} followed by a function of ω^{-4} .

Fig. 2 shows the optical reflectance spectra of pure

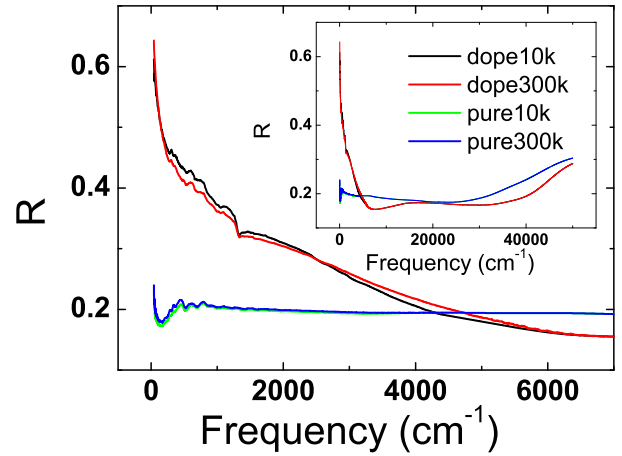


FIG. 2: (color online) Frequency dependence of reflectance spectra of pure and boron-doped diamond from 40 cm^{-1} to 6400 cm^{-1} at different temperature. The inset is the whole spectra from 40 cm^{-1} to 50000 cm^{-1} .

and doped samples measured at 10 K and 300 K. A weak temperature dependence was found for the doped sample. The reflectance in the frequency range of 150 - 2400 cm^{-1} increases somewhat with decreasing temperature, however, its reflectance below 150 cm^{-1} or above 2400 cm^{-1} decreases with decreasing temperature. Above 6400 cm^{-1} the reflectance spectra are temperature independent. As for the pure diamond sample, it shows featureless changing over a broad frequency range. The increase above 30000 cm^{-1} is ascribed to the onset of interband transition. The low- ω reflectance decreases slightly with decreasing temperature, being consistent with the insulating characteristic. As revealed clearly in this figure, the major difference between the pure and B-doped diamonds is a substantial increase of the low frequency reflectance (below ~ 5000 cm^{-1}) for the doped sample. The low- ω spectral weight was transferred from high frequency range above ~ 5000 cm^{-1} as well as in the interband transition region. So, the reflectance data illustrate clearly that B-doping leads to formation of electronic states at low energies. Metallic conduction can be caused when those states are enough to form a band crossing the Fermi level.

Fig. 3 shows the conductivity spectra in a broad frequency range. For the pure diamond sample, the spectral weight at low frequency is extremely low. A sharp increase in $\sigma(\omega)$ appears at frequency exceeding 30,000 cm^{-1} . This is due to the interband transition from valence band to conduction band. For the B-doped sample, on the other hand, an increase of spectral weight at frequency below 7000 cm^{-1} is evident. In the meantime, the onset of interband transition shifts somewhat to higher frequencies. Notably, the low energy excitations do not form a Drude peak. The conductivity was severely suppressed at low frequency, resulting in a broad peak centered at $\sim 3,000$ cm^{-1} (0.38 eV). This means that the states induced by B-doping are still highly localized.

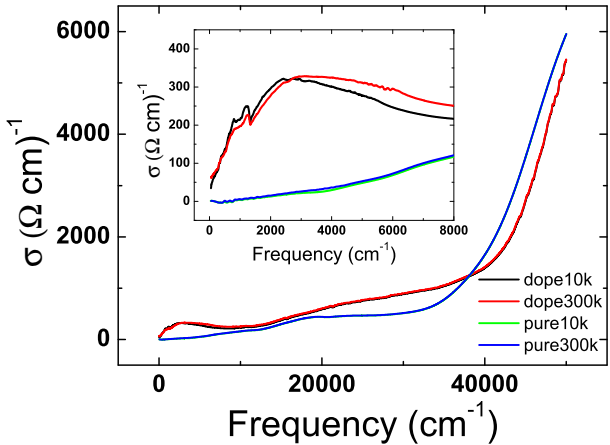


FIG. 3: (color online) The optical conductivity spectra of pure and boron-doped diamond over broad range of frequencies. The inset is the expanded spectra from 40 cm^{-1} to 8000 cm^{-1} .

We noticed that the peak energy corresponds well to the boron acceptor levels locating at 0.38 eV from the top of valence band as determined from many other experimental probes.[7, 16] So, it just corresponds to the interband transition from the top of the valence band to the impurity states.

Based on the above experimental data, we can draw following schematic picture for the evolution of the electronic states for B doping diamond as shown in Fig. 4. The pure sample is a standard semiconductor with the valence band completely filled and conduction band completely empty. The Fermi level locates close to the top of the valence band (Fig. 4(a)). B-doping creates the acceptor impurity states (near the Fermi level) with a binding energy of 0.38 eV. When the doping levels are low, those energy levels are isolated, and the impurity states are completely localized (Fig. 4(b)). As the boron concentration increases, the impurity energy levels broaden and form a band. At high enough doping level, the impurity band may overlap with the top states of valence band because of their very close energies (Fig. 4(c)). Metallic conduction could be formed as long as the impurity band crosses the Fermi level. Additionally, because the holes are created in the valence band, a slight downward shift of Fermi level likely occurs, which can explain the observed energy shift of interband transitions. Obviously, for our polished B-doped sample, it corresponds to the states between Fig. 4 (b) and (c).

The above picture shares some similarity with the high temperature cuprate superconductors which are doped Mott insulators. For the undoped parent compound, the lowest interband transition is the charge transfer excitations, that is, the transition from occupied O_{2p} band to the empty upper Hubbard band of Cu 3d electrons. When carriers, for example holes, are doped into the compound, they starts to create some midgap states within the charge transfer gap. In optical spectra, one can observe a transfer of the spectral weight from the in-

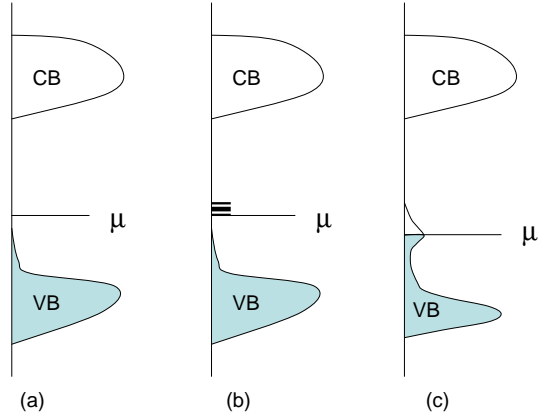


FIG. 4: (color online) A schematic diagram for the evolution of the electronic structure of diamond with B-doping. (a) The pure diamond is a typical semiconductor. The chemical potential is close to the top of the valence band. (b) Boron-doping introduces acceptor impurity energy levels near the top of the valence band. (c) With increasing boron doping, the boron impurity levels form a band, and may overlap with the top of the valence band. Metallic conduction occurs as long as the impurity band crosses the chemical potential.

terband transition to the mid-infrared band. With increasing doping, the mid-infrared band shifts to lower frequency and finally merges with the Drude band that appears when the concentration is higher than the critical x_c for insulator-metal transition. Here, in the boron-doped diamond system, the mid-gap states are just from those boron acceptor impurity band. When the impurity band crosses the Fermi level, the compound can becomes metallic. We believe that the superconductivity originates from this impurity band. Baskaran proposed that the impurity band has very strong electron correlation, which could be split into lower and upper subbands, in addition to some extra mid-gap states. If this is the case, one would expect to see another interband transition from occupied states to the upper Hubbard impurity band for boron doped sample. The present experimental result does not support this scenario because no such interband transition is observed.

Besides the change in electronic states with B-doping, there also exists important difference between pure and doped sample with regard to phonon spectra. We noticed that the doped sample has a peculiar structure at about 1330 cm^{-1} in reflectance and conductivity spectra, while the pure sample does not show any anomaly at this frequency. In the Raman spectra of pure diamond, a very sharp zone-center phonon peak was observed at 1332 cm^{-1} .[17] This Raman mode is obviously forbidden in infrared as the reflectance is featureless in this particular region. As the boron atoms substitute for carbon in crystal structure, the distortion of vibrational eigenvectors brings nonzero moments of electronic dipoles for most vibrational modes. So the exceptional feature in doped one at $\sim 1330\text{ cm}^{-1}$ should be explained as the

activated infrared-forbidden mode by impurity.

We noticed that this phonon mode has an anti-resonance characteristic in the conductivity spectrum, namely, the feature looks more like an asymmetric dip than a peak in the electronic background of conductivity spectrum. Usually, a phonon displays a peak structure centered at its characteristic frequency. The peak can be asymmetric (Fano lineshape) due to an interaction of lattice with the electrons. The rather obvious anti-resonance feature is an indication of the strong electron-phonon coupling in the compound. Such a phenomenon is more commonly seen in organic conductor or superconductors as a result of significant electron-molecular vibration coupling[18, 19]. The presence of such peculiar phonon structure unambiguously illustrates the very strong electron-phonon coupling in present doped diamond sample. In fact, the strong coupling of electrons with such mode and its significant effect on the superconductivity in B-doped diamond has been addressed in a number of theoretical studies recently.[10, 11, 12, 13] Our infrared response study provides experimental evi-

dence for the strong coupling of electrons with this mode.

In summary, we have performed optical reflectance measurements on polished surfaces of both pure and boron-doped diamond films grown by a hot-filament chemical vapor deposition method. Significant difference has been found from the reflectance and conductivity spectra in pure and boron-doped samples. The study revealed clearly the formation of an acceptor impurity states near the top of the valence band with boron doping. It is suggested that this impurity band could overlap with the valence band at high enough doping, and the superconductivity is originated from this impurity band. The study also revealed the impurity's effect on phonon vibration modes and a very strong electron-phonon coupling in the doped compound.

We thank J. Y. Shen for her help in experiment. This work was supported by the Ministry of Science and Technology of China (973 project No. 2006CB601002), the National High Technology Development Program of China (Grant No. 2002AA325090), and the National Science Foundation of China.

[1] W. C. Walker and J. Osantowski, Phys. Rev. **134**, A153 (1964).
[2] W. Saslow, Phys. Rev. Lett. **16**, 354 (1966).
[3] H. Shiomi, Y. Nishibayashi, and N. Fujimori, Jpn. J. Appl. Phys. **30**, 1363 (1991).
[4] J. P. Lagrange, A. Deneuville, and E. Gheeraert, Diam. Relat. Mater. **7**, 1390 (1998).
[5] M. Werner, O. Dorsch, H. U. Baerwind, E. Obermeier, L. Haase, W. Seifert, A. Ringhandt, C. Johnston, S. Romani, H. Bishop, and P. R. Chalker, Appl. Phys. Lett. **64**, 31 (1994).
[6] E. Bustarret, E. Gheeraert, and K. Watanabe, Phys. Stat. Sol.(a) **199**, 9 (2003).
[7] J. Nakamura, E. Kabasawa, and N. Yamada, Phys. Rev. B. **70**, 245111, (2004).
[8] E. A. Ekimov, V. A. Sidorov, E. D. Bauer, N. N. Mel'nik, N. J. Curro, J. D. Thompson, and S. M. Stishov, Nature **428**, 542 (2004).
[9] Y. Takano, M. Nagao, I. Sakaguchi, M. Tachiki, T. Hatano, K. Kobayashi, H. Umezawa, and H. Kawarada, Appl. Phys. Lett. **85**, 2851 (2004).
[10] L. Boeri, J. Kortus, O. K. Andersen, Phys. Rev. Lett. **93**, 237002 (2004).
[11] K. W. Lee and W. E. Pickett, Phys. Rev. Lett. **93**, 237003 (2004).
[12] X. Blase, Ch. Adessi, and D. Connetable, Phys. Rev. Lett. **93**, 237004 (2004).
[13] H. J. Xiang, Z. Li, J. Yang, J. G. Hou, and Q. Zhu, Phys. Rev. B **70**, 212504 (2004).
[14] G. Baskaran, cond-mat/0404286, cond-mat/0410296.
[15] C. C. Homes, M. Reedyk, D.A. Crandles, and T. Timusk, Appl. Opt. **32**, 2976 (1993).
[16] A. S. Barnard, S. P. Russo, and I. K. Snook, Phil. Mag. **83**, 1163 (2003).
[17] J. W. Ager III, W. Walukiewicz, M. McCluskey, M. A. Plano, and M. I. Landstrass, Appl. Phys. Lett. **66**, 616 (1995).
[18] C. S. Jacobsen, *Semiconductors and Semimetals*, Vol 27, ed. E. Conwell (London: Academic) ch. 5, p. 293 (1988).
[19] N. L. Wang, H. Mori, S. Tanaka, J. Dong, and B. P. Clayman, J. Phys.: Condens. Matter **13**, 5463 (2001).